Seismic characteristics and distribution of volcanic intrusions and hydrothermal vent complexes in the Vøring and Møre basins

S. PLANKE,[1,2] T. RASMUSSEN,[1] S. S. REY[1] and R. MYKLEBUST[3]

[1] *Volcanic Basin Petroleum Research (VBPR), Oslo Research Park, 0349 Oslo, Norway (e-mail: planke@vbpr.no)*
[2] *Physics of Geological Processes, University of Oslo, PO Box 1048 Blindern, 0316 Oslo, Norway*
[3] *TGS-NOPEC, Baarsrudveien 2, 3478 Nærsnes, Norway*

Abstract: A voluminous magmatic complex was emplaced in the Vøring and Møre basins during Paleocene/Eocene continental rifting and break-up in the NE Atlantic. This intrusive event has had a significant impact on deformation, source-rock maturation and fluid flow in the basins. Intrusive complexes and associated hydrothermal vent complexes have been mapped on a regional 2D seismic dataset (*c*.150 000 km) and on one large 3D survey. The extent of the sill complex is at least 80 000 km^2, with an estimated total volume of 0.9 to 2.8×10^4 km^3. The sheet intrusions are saucer-shaped in undeformed basin segments. The widths of the saucers become larger with increasing emplacement depth. More varied intrusion geometries are found in structured basin segments. Some 734 hydrothermal vent complexes have been identified, although it is estimated that 2–3000 vent complexes are present in the basins. The vent complexes are located above sills and were formed as a direct consequence of the intrusive event by explosive eruption of gases, liquids and sediments, forming up to 11 km wide craters at the seafloor. The largest vent complexes are found in basin segments with deep sills (3–9 km palaeodepth). Mounds and seismic seep anomalies located above the hydrothermal vent complexes suggest that the vent complexes have been re-used for vertical fluid migration long after their formation. The intrusive event mainly took place just prior to, or during, the initial phase of massive break-up volcanism (55.0–55.8 Ma). There is also evidence for a minor Upper Paleocene volcanic event documented by the presence of 20 vent complexes terminating in the Upper Paleocene sequence and the local presence of extrusive volcanic rocks within the Paleocene sequence.

Keywords: volcanic rifted margins, volcanic basins, hydrothermal vent complexes, sill complexes

Volcanic processes and deposits may have a strong impact on the structure and geodynamic development of continental margins and associated sedimentary basins. The identification of volcanic deposits and the evaluation of their impact on the margin history are, thus, two important aspects of petroleum exploration of continental rifted margins. Significant attention has, over the past decade, been devoted to studies of extrusive processes and deposits on volcanic rifted margins (e.g. Eldholm *et al*. 1989; Menzies *et al.* 2002; White *et al*. 2003). However, petroleum explorationists will commonly encounter intrusive complexes before they encounter extrusive volcanic rocks when they move from shallow-water to deep-water areas. Deep-water explorationists, therefore, need to know how to recognize, interpret and risk-evaluate intrusive complexes.

The frontier Vøring and Møre basins off mid-Norway are classical examples of intruded volcanic basins located on a rifted volcanic margin (e.g. Skogseid *et al*. 1992; Skogly 1998; Berndt *et al*. 2000; Brekke 2000; Gernigon *et al*. 2003). The volcanic activity in these basins was associated with Late Paleocene rifting and continental break-up in the NE Atlantic. Similar intrusive basin provinces are located along the entire European NE Atlantic margin (e.g. Gibb & Kanaris-Sotiriou 1988; Bell & Butcher 2002; Smallwood & Maresh 2002) and onshore in central-east Greenland (e.g. Larsen & Marcussen 1992; Price *et al*. 1997).

Sill complexes may have a major impact on basin history and petroleum systems. The short-term effects during magma emplacement include deformation, uplift, heating of host rock, metamorphism, petroleum maturation and boiling of host-rock fluids, possibly leading to the formation of hydrothermal vent complexes. The long-term effects include focused fluid flow and compartmentalization, armouring of the sedimentary sequence by mechanically strong dolerite and hornfels, and differential compaction. These systems are being studied by integrated seismic imaging and interpretation (NE Atlantic margins), fieldwork (Karoo basin, South Africa; central-east Greenland) and geodynamic modelling (magma emplacement, heat transport, maturation and boiling) activities (Svensen *et al*. 2003; Jamtveit *et al*. 2004; Malthe-Sørenssen *et al*. 2004).

The aim of this paper is to document the nature and distribution of intrusive complexes and associated hydrothermal vent complexes on the mid-Norway margin. These results are used to provide constraints on the geological processes and petroleum implications of intrusive volcanism (e.g. Jamtveit *et al*. 2004; Malthe-Sørenssen *et al*. 2004). The Vøring and Møre basins are well suited for this research, as Early Tertiary sill complexes are present in large parts of the Cretaceous basins. In addition, extensive high-quality seismic reflection data and other geophysical data are currently available in these basins.

Terminology

Volcanic basins are sedimentary basins with a significant quantity of primary emplaced volcanic rocks.

Pierced basins are sedimentary basins with many piercement structures, such as mud volcanoes and hydrothermal vent complexes.

Sheet intrusions are tabular igneous bodies, such as sills, dykes, and laccoliths.

Sills are tabular igneous intrusions that are dominantly layer parallel. They are commonly sub-horizontal. Sills may locally have transgressive segments, i.e. segments that cross-cut the stratigraphy.

PLANKE, S., RASMUSSEN, T., REY, S.S. & MYKLEBUST, R. 2005. Seismic characteristics and distribution of volcanic intrusions and hydrothermal vent complexes in the Vøring and Møre basins. *In*: DORÉ, A. G. & VINING, B. A. (eds) *Petroleum Geology: North-West Europe and Global Perspectives—Proceedings of the 6th Petroleum Geology Conference*, 833–844. Published by the Geological Society, London.

Hydrothermal vent complexes are pipe-like complexes formed by fracturing, transport and eruption of hydrothermal fluids and sediments.

Data and method

Database

The project database consists of more than 1100 regional 2D seismic profiles, with a length of *c*. 150 000 km and one 3D-cube covering *c*. 2000 km^2 (Fig. 1). In addition, high-pass filtered and gridded high-quality ship-track gravity data and high-resolution aeromagnetic data were available for most of the study area (Planke & Myklebust 1999). Public-domain bathymetry (e.g. IBCAO), satellite gravity (Sandwell & Smith 1997) and magnetic data (Verhoef *et al*. 1996) were also used. Few wells are drilled in the outer Vøring and Møre basins. Only one good well-tie to the imaged sill complexes exists (6607/5-2; Fig. 2). Well 6607/12-1, near the Nordland Ridge, was drilled through a hydrothermal vent complex and a comprehensive analysis of this well has recently been completed (e.g. Svensen *et al*. 2003). In addition, wells 6406/3-2, 6406/6-1, 6406/11-1, 6506/11-2 and 6507/2-1 were used to calibrate the interpretations.

Method

Data integration and interpretation were mainly carried out in a seismic workstation environment. Most seismic profiles were decimated and re-sampled to 8 ms to increase the computer performance. 50 km to 100 km high-pass filtered gravity and aeromagnetic data were converted to pseudo-horizons and loaded into the workstation software to facilitate qualitative integrated seismic–gravity–magnetic interpretation. Seismic modelling and re-processing activities and potential-field modelling studies complemented the qualitative interpretation.

Sill complex interpretation

Interpretation of sill intrusions differs from conventional methods for time horizon mapping. Sill interpretation requires determination of lithology. Moreover, sill intrusions may split into several units or several units may merge into one unit. Sills can transgress

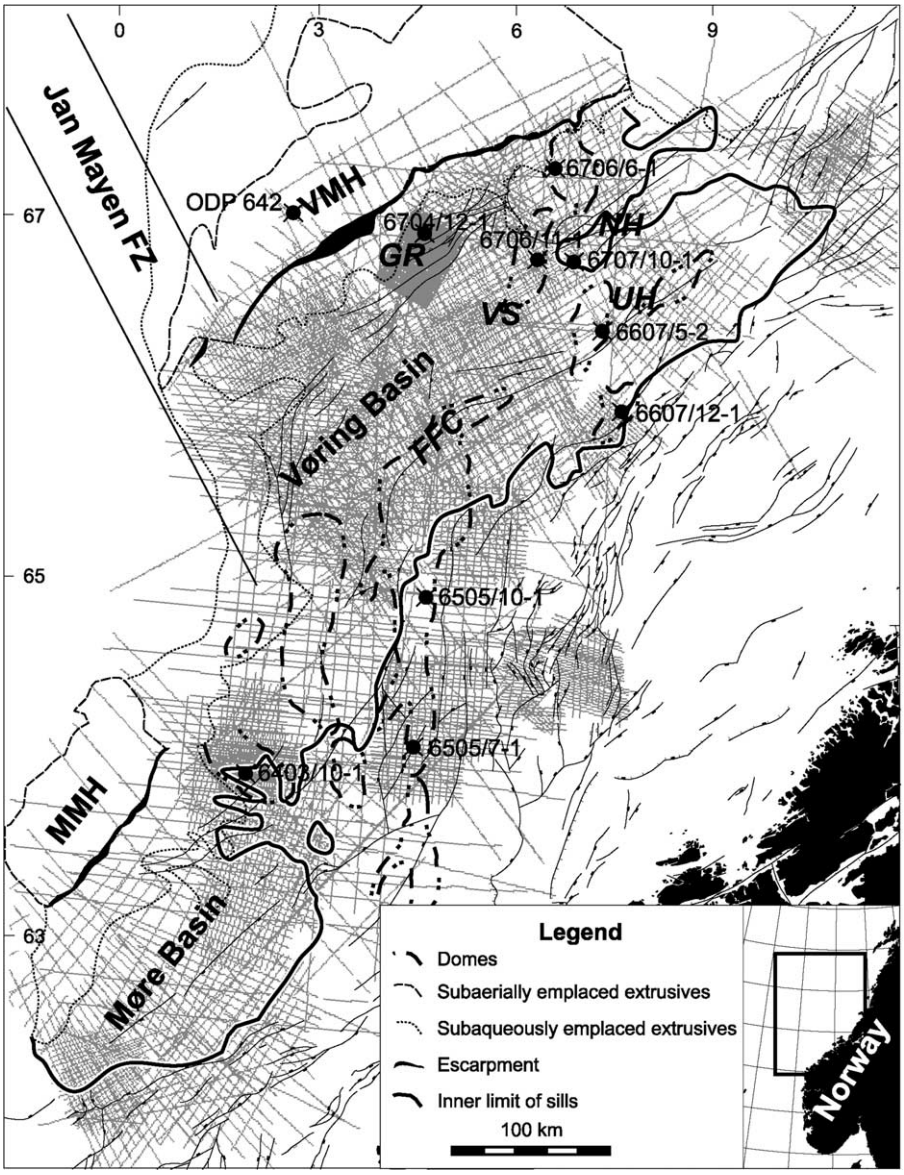

Fig. 1. Location map showing interpreted seismic database and structural framework. FFC, Fles Fault Complex; GR, Gjallar Ridge; MMH, Møre Marginal High; NH, Nyk High; UH, Utgard High; VS, Vigrid Syncline; VMH, Vøring Marginal High. Inner limit of sill complex from this study. Volcanic extrusive domains from Berndt *et al.* (2001); structural elements from Blystad *et al.* (1995).

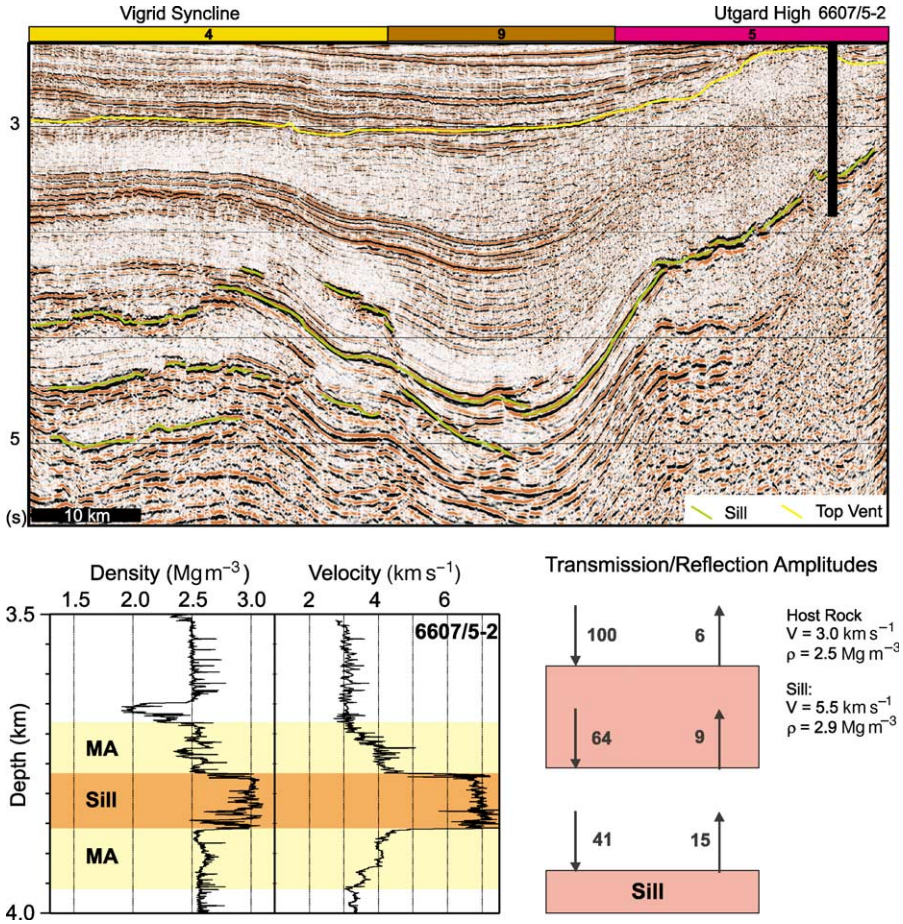

Fig. 2. Seismic profile through well 6607/5-2 on the Utgard High. The middle sill is well imaged on the velocity and density logs and can be correlated with a high-amplitude reflection on the seismic profile extending into the Vigrid Syncline. However, the deep sill is poorly imaged on the seismic profile. This may partly be due to the low amplitude of the wave reflected from a sill when it has to travel through another sill in the overburden (the amplitude of the reflected wave from the top of sill 1 is 5–6 times higher than the amplitude of the reflected wave from the top of sill 2).

(i.e. move up or down in the stratigraphy) and may contain holes. In this study a combination of interpretation methods has been used: (1) interpretation of sill reflections, (2) 3D voxel visualization, (3) seismic facies analysis; and (4) mapping of surfaces.

The following main criteria were used to interpret a seismic event as a sill reflection: (1) high amplitude; (2) local transgression; (3) saucer-shape; and (4) abrupt terminations. A reflection is identified as a possible sill reflection if it is a high-amplitude event. If the event transgresses, is saucer-shaped and/or terminates abruptly, then the reflection is interpreted as a probable sill reflection. An event may also be interpreted as a sill reflection if it can be correlated with interpreted sills on crossing profiles. The reliability of the interpretation depends on how well the criteria are satisfied. In addition, borehole calibration, magnetic data, 3D visualization geometries and pre-stack seismic analyses were used to increase the reliability of the seismic interpretation. An example of a sill complex interpreted by this method is shown in Figure 3. Note that only sill reflections interpreted with a high reliability are used in this study and the mapping, thus, provides a conservative estimate of the sill distribution. All picked sill horizons were merged and the shallowest sill at each location was used to make a gridded surface.

Sill complexes are well suited for 3D visualization methods because of the high seismic amplitude and complex shape of the

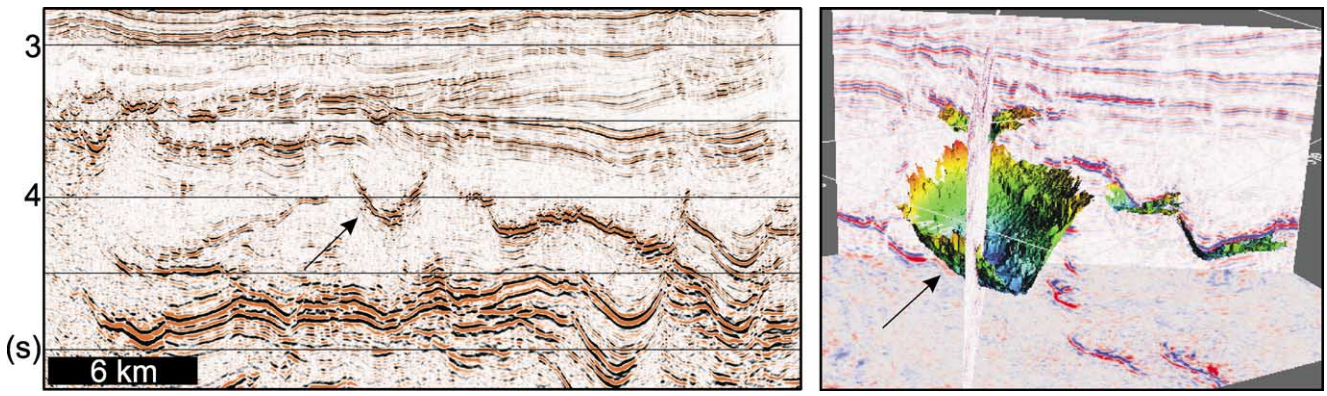

Fig. 3. 3D visualization of the Gleipne Sill Complex. The saucer-shaped sill (right) is 3 × 4 km wide and 0.5 km high. The saucer-shaped sill complex (arrow) is also nicely imaged on crossing 2D profiles (left).

sill reflections (Fig. 3). However, the uppermost intrusions often inhibit deep imaging, making it difficult to visualize the entire complex. In this study, the software VoxelVision was used to study the 3D aspects of the Gjallar and Gleipne sill complexes in the outer Vøring Basin.

Identified sill reflections were described and mapped using the concept of seismic facies analysis, a method that was originally described by Vail & Mitchum (1977). Seismic facies analysis is the description and geological interpretation of seismic reflection parameters, including configuration, continuity, frequency and interval velocity. This method includes the definition and mapping of seismic facies units. A seismic facies unit is a mappable, three-dimensional group of seismic reflections, whose reflection parameters differ from the adjacent facies units. The traditional use of seismic facies analysis is in sedimentary environments, but the method is also used in volcanic environments (e.g. Planke *et al.* 2000). Seismic facies analysis is also a suitable method for mapping of sill intrusions (Skogly 1998), as the sills show a wide range of geometries and reflection parameters.

The seismic facies units ('sill facies units') were identified on the seismic profiles and plotted on a map. The boundaries of the sill facies units are not obvious in some cases, as diffuse boundaries and overlaps of facies units may occur. If overlapping sill reflections showed different seismic facies, then the dominating facies unit was plotted on the map. If facies units merged, then the limit between the facies units was put at the centre of the transition zone.

Hydrothermal vent complexes

Two main intra-Tertiary horizons were interpreted regionally based on seismic characteristics. These are the Top Vent and the Top Mound horizons. The Top Vent horizon was defined at key locations where the upper part of the hydrothermal vent complexes is well defined (Figs 4 and 5). Care was taken to keep to the same stratigraphic level between the vent complexes. The Top Mound horizon is characterized by small, mounded highs, seen as vertical series of convex reflections and generally terminating at a consistent stratigraphic level. The mounded highs are located above the upper part of hydrothermal vent complexes or above the termination of deep-seated faults. The Top Mound horizon was picked at a well-defined, laterally continuous trough at the uppermost part of the convex reflection package, where the mound showed the greatest positive relief. The Top Mound horizon was subsequently correlated between the well-defined picks. A consistent stratigraphic level was maintained throughout the interpretation. The Top Mound horizon is most distinct in the central Vøring Basin. Here, it is identified as a high-amplitude, continuous reflection defining the base of a generally low-amplitude sequence characterized by numerous, steep, small-offset normal faults. The Top Mound horizon was not interpreted in the central and southern Møre Basin, as it is difficult to identify here. Finally, a Base Vent Horizon was interpreted locally. Horizon and isochron maps were subsequently generated and then high-pass filtered (25 and 50 km cut-off frequencies).

The seismic characteristics of each interpreted hydrothermal vent complex and the surrounding strata were entered into a pseudo-well database. The following seismic features were interpreted (Figs 4 and 5): (1) the geometry and size of the upper part of the vent complex (eye-, crater- or dome-shaped); (2) the nature of overlying reflections (mounded; high-amplitude events; disturbed events); (3) the nature of underlying reflections (inward- and outward-dipping events around the chimney; disrupted seismic data; high-amplitude events); and (4) the presence and nature of the underlying sill complex.

The sill complex

Three sills were penetrated by well 6607/5-2 on the Utgard High (Fig. 2). The uppermost sill is a 2 m thick dolerite in late Campanian claystones at a depth of 3419 m. A 91 m thick sill was reached at a depth of 3792 m, intruded into altered claystones of the Campanian Shetland Group. The well terminated 50 m into a third sill below Turonian sandstones (Berndt *et al.* 2000). Sonic

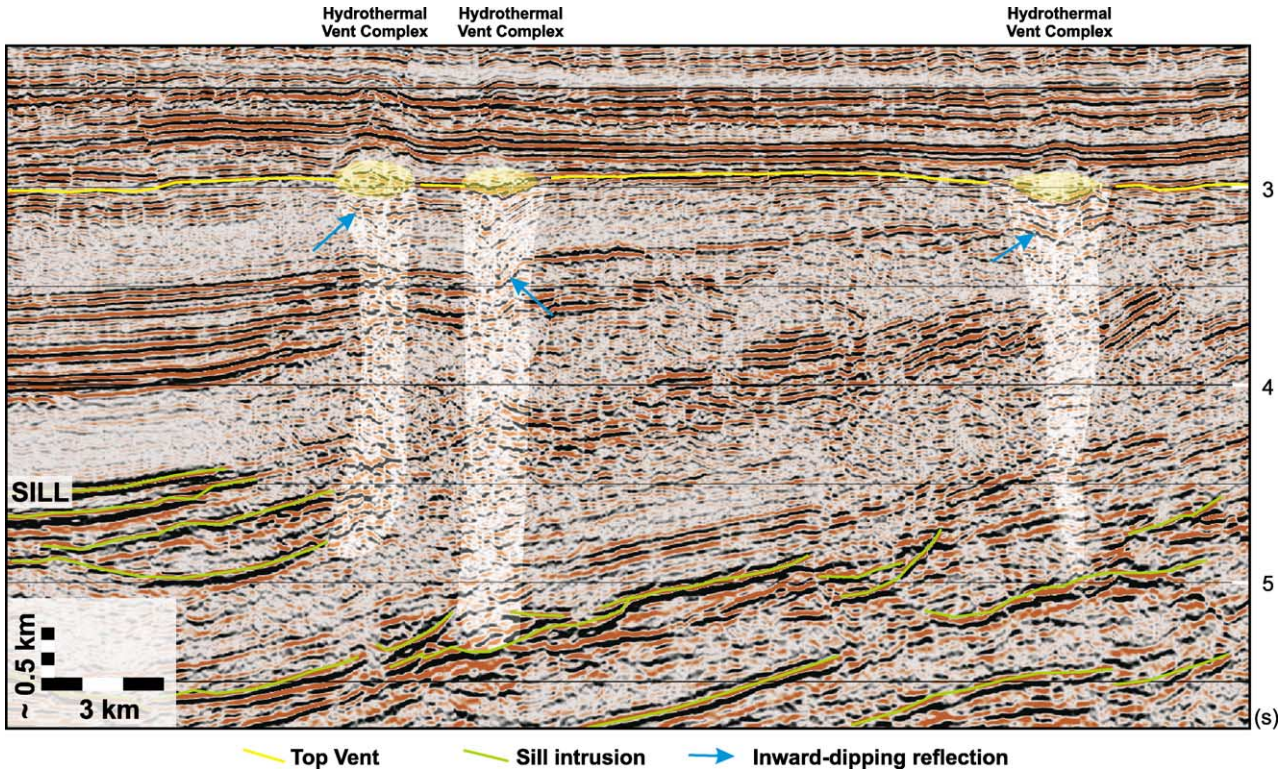

Fig. 4. Seismic example of hydrothermal vent complexes in the central Vøring Basin. Note the eye-shaped upper part of the vent complexes, the doming of the overburden, and discontinuous, partly inward-dipping reflections around the chimney. From Jamtveit *et al.* (2004).

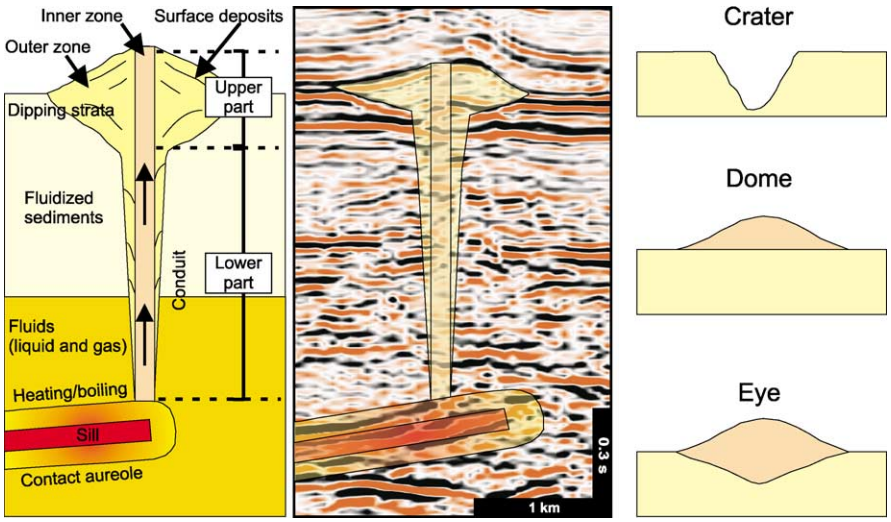

Fig. 5. Sketch and seismic example of a hydrothermal vent complex. The complex consists of an upper and a lower part. The upper part is crater-, dome- or eye-shaped and is connected to the termination of a sill by a cylindrical conduit zone with disturbed seismic data in the lower part.

logs from the well show that the middle sill has an average velocity of 7.0 km s^{-1} (Fig. 2), which is very high compared with the average sill p-wave velocity of 5.5 km s^{-1} for >80 intrusions drilled West of Shetland (Skogly 1998; Berndt *et al*. 2000). The middle intrusion is clearly visible on a seismic section through the well and can be correlated with a sill complex in the Vigrid Syncline >100 km to the west (Fig. 2). The well provides a good tie to the sill complexes in the Vøring Basin, and improves the reliability of the seismic interpretation. Note that the upper and lower sills drilled by well 6607/5-2 are not well imaged on the seismic profile. The uppermost sill is too thin to be imaged. The lowermost sill is probably poorly imaged due to large transmission losses of reflected energy crossing the high-impedance boundaries between the middle sill and the host rock four times (Fig. 2).

Sill intrusions have been interpreted regionally on the seismic data in the Møre and Vøring basins. Two seismic type-profiles across the central Møre Basin and the southern Vøring Basin are shown in Figure 6. The intruded area has a width of 50–150 km

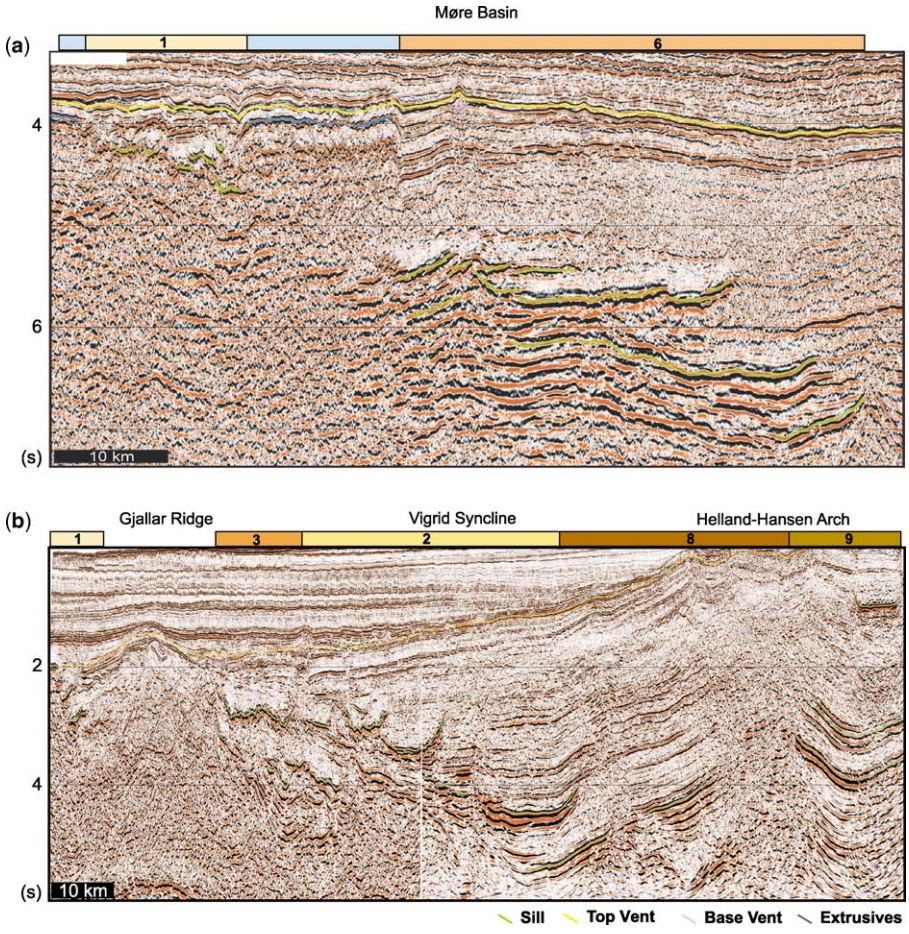

Fig. 6. Seismic examples of sill complexes and sill facies units in (**a**) the Møre and (**b**) Vøring basins. Note the clear increase in the size of the saucers with depth. Also note how the shallow sills are short and rough, whereas the deep sills are smoother and more continuous.

and a length of 65 km, with a total extent of 82 000 km^2 (Fig. 7). The southern part of the sill complex is defined by the UK border, whereas the northern extent of the sill complex corresponds to the transition between the Vøring and Lofoten margins. The western extent of the sill complex is uncertain as the Cretaceous basin is poorly imaged here due to the presence of overlying volcanic extrusive rocks. The basin and the sill complex probably extend westward at least to the regional escarpments, but sills have also been interpreted west of the Faroe–Shetland Escarpment on a few high-quality profiles across the Møre margin (Planke & Alvestad 1999). The eastern extent of the sill complex is fairly well defined, except in the very northern and southern regions where high-amplitude events are associated with major pre-Cretaceous faults. These high-amplitude events can be interpreted as sills, but the seismic database is not sufficiently dense to reliably interpret sills in these regions. Finally, note that break-up-aged volcanic rocks of the Vestbrona Formation have been dredged near the Norwegian coast off Kristiansund (Bugge *et al.* 1980), showing that the eastward extent of the intrusive complexes can locally be much greater than currently mapped.

The sills were emplaced at progressively deeper levels toward the east. Sills in the central Møre and Vøring basins show a stepping pattern in a southeasterly direction, whereas sills along the Vøring Transform Margin (VTM) reveal the same stepping pattern in a northeasterly direction (Figs 6 and 7). The width of the sill complex and the extrusive complex is much smaller in the northern Møre Basin than elsewhere along the margin. Further, note that sills cannot be identified in several structural highs such as the Gjallar Ridge, the Nyk High and the Utgard High.

The sill thickness and the number of sills are difficult to map. The thickness of a sill can be measured from the peak-to-trough length. The Rayleigh vertical resolution limit is $\lambda_d/4$ where λ_d is the dominant wavelength. However, commonly a $\lambda_d/2$ thickness is required to identify confidently the top and bottom reflection of a thin layer. The detection limit is more difficult to quantify, but is approximately $\lambda_d/10$. The dominant wavelength of a sill

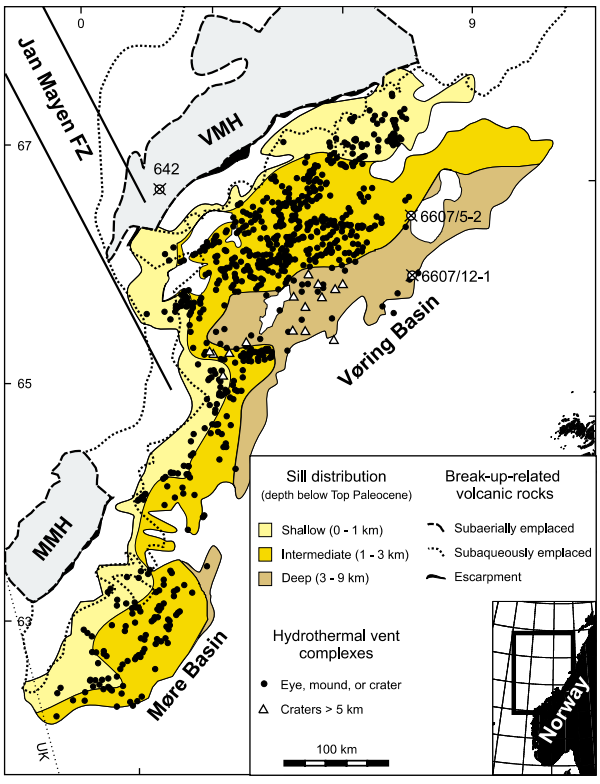

Fig. 7. Distribution of sill intrusions and location of hydrothermal vent complexes in the Vøring and Møre basins. MMH, Møre Marginal High; VMH, Vøring Marginal High; FZ, Fracture Zone.

with p-wave velocity of 5.5 km s^{-1} is 183 m. A sill, thus, needs to be between 46 m and 91 m to be resolved and >18 m thick to be detected under perfect imaging conditions. However, complicating factors, such as offset-dependent tuning, complex 3D geometries of the sills, velocity increase in the metamorphic aureole and structural variations in the overburden, commonly make it difficult to obtain these resolution criteria. Field data from east-central Greenland and the Karoo show that extensive sills have typical thicknesses of 50–150 m and are, thus, in a thickness range that cannot commonly be resolved.

The most severe problem for estimating the thickness and total volume of the mid-Norway sill complex is related to the sub-sill imaging problem. It is often possible to interpret several sill layers (e.g. Figs 3, 4 and 6), but the continuity of the deeper sills is commonly lost when the thickness and/or number of overlying sills increases (e.g. Fig. 6a). In addition, high-amplitude seismic events below the uppermost sill are commonly not primary events, but rather peg-leg multiples or converted waves. Field data show that many levels of intrusions are common in volcanic basins (e.g. the Karoo and central-east Greenland) and this is also probably the situation in large parts of the Vøring and Møre basins. Exceptions are in regions with structural highs and in the westernmost parts when the deep sill complex dies out.

A minimum estimate of the average total thickness of the intruded basin is 100 m, whereas a more likely conservative average thickness estimate is 300 m. The extent of the mapped sill complexes is at least 80 000 km^2, whereas the sills are probably also present below the Inner Flows region, which has an area of 13 000 km^2. Based on these numbers, the total volume of the sill complex in the Vøring and Møre basins is in the order of 0.9×10^4 km^3 to 2.8×10^4 km^3.

It is difficult to identify several phases of magma emplacement based on the seismic interpretation of the sill complex. Individual sill reflections can be correlated for tens and hundreds of kilometres, suggesting large-volume intrusive events. Furthermore, no clear cross-cutting relationships are observed. There are two main potential source areas for the intruded magma: (1) weak fault zones along major deep-seated structures within the basins; and (2) fissures near the break-up axis west of the basins. In addition, extruded lava may intrude into unconsolidated sediments (e.g. Planke *et al.* 2000). Modelling of high-amplitude magnetic anomalies in the central part of the Møre Basin and in the southern part of the Vøring Basin (Rån Ridge area) shows that dyke swarms on the flanks of deep-seated structural highs can explain the observed magnetic anomalies. Field data from central-east Greenland show that Mesozoic faults are used as conduits for magma transport and that a large sill complex with several levels was emplaced simultaneously (e.g. Månedalen Fault Complex; Planke *et al.* 1999). These observations suggest that the magma source area was commonly local, i.e. weakness zones within the basin.

Sill facies units

Nine sill facies units have been defined and mapped in the Møre and Vøring basins (Fig. 8; Table 1). There are two main groups: (1) layer parallel and (2) saucer-shaped. These groups are subdivided into six seismic facies units based on the smoothness, size, continuity and depth from the palaeosurface of the interpreted sill reflections. In addition, a transitional facies unit, a Slightly Saucer-Shaped unit, has been defined. Finally, two more sill facies units have been defined, a Planar Transgressive facies unit and a Fault Block facies unit.

The Møre and Vøring basin sill complexes can be divided into three regions, the Vøring Basin, the VTM and the Møre Basin sill complexes, depending on the direction of the deepening of the top sill reflection. Three facies units are interpreted in the Møre Basin, with an outer zone of Shallow Intrusions, a central zone of Slightly Saucer-Shaped sills and an inner zone of Smooth Layer-Parallel

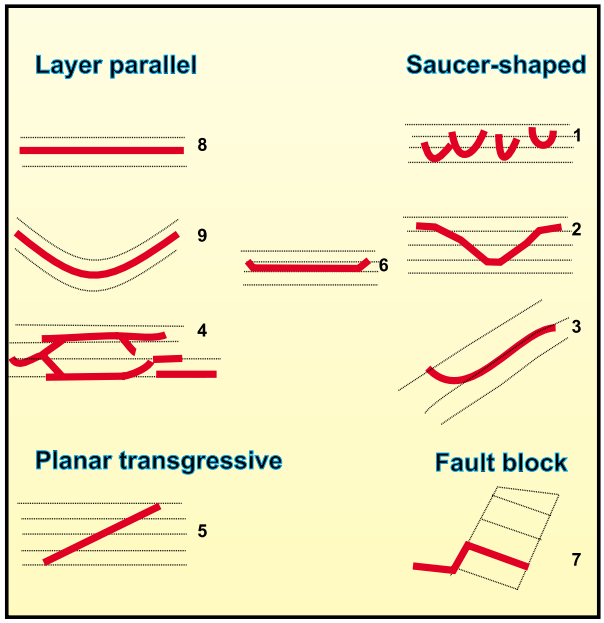

Fig. 8. Sketch showing the configuration of identified sill facies units (see Table 1 for description).

sills (Fig. 6a). A more complicated sill facies unit distribution is present in the Vøring Basin. The outer region is dominated by Shallow Intrusions and Rough Saucer-Shaped sills, with no sills in the central parts of the Gjallar High (Fig. 6b). The central Vigrid Syncline is dominated by Layer-Parallel Rough sills, which merge into a Planar Transgressive sill facies unit towards the Fles Fault Complex (Fig. 2). Layer-Parallel and Basin-Parallel facies units dominate the inner parts of the basin (Fig. 6b). The VTM Sill Complex is located along the Jan Mayen Fracture Zone. In the north it merges with the Vøring Basin Sill Complex and is adjacent to the Møre Basin Sill Complex in the south. The VTM Sill Complex has a stepping pattern, down to the NE and SE north and south of the Jan Mayen Fracture Zone, respectively (Fig. 7).

Hydrothermal vent complexes

Horizon mapping

The Top Vent horizon was interpreted over most of the study area. However, it was not interpreted west of the Vøring and Faroe–Shetland escarpments or on the Lofoten Margin, where no hydrothermal vent complexes were identified. In the outer parts of the basins the horizon terminates near the extrusive Inner Flows. However, SW in the Vøring Basin and in the central Møre Basin, the Top Vent horizon continues seaward above two regions with interpreted extrusive deposits in the Paleocene sequence. In these regions the Top Vent horizon terminates against the Inner Flows near the escarpment, following the Top Paleocene horizon interpreted by Hjelstuen *et al*. (1999). In the outer central Møre Basin one observes a group of 20 vent complexes, whose upper parts are located at a deeper stratigraphic level than the Top Vent horizon.

The Top Mound horizon was only interpreted in the Vøring Basin. It is limited to the NW by the Vøring–Lofoten margin transition and terminates against the Vøring Escarpment in the West Vøring Basin. At the Vøring Transform Margin, the horizon terminates against the Jan Mayen Fracture Zone. There is no eastward termination within the dataset. In the central and southern Møre Basin the mound structures were not found at a consistent stratigraphic level and the horizon was not interpreted.

Table 1. Sill seismic facies units

	Unit	Description
(1)	Shallow Intrusions	A narrow saucer-shaped geometry with a rough seismic character (Fig. 6). The facies unit is found along the whole margin, but is locally absent or masked by overlying lava flows. It is located at shallow depths below the palaeosurface adjacent to the landward termination of the lava flows and merges gradually with the deeper intrusions. Shallow layer-parallel peperitic sills are also classified as Shallow Intrusions.
(2)	Saucer-Shaped Rough	Saucer-shaped sills with a rough seismic character (Fig. 6b). The facies unit is distinguished from the Shallow Intrusions by a deeper deposition level and a greater width of the saucers. The unit is located landward of the Shallow Intrusions at 0.5–1.5 s depth below the palaeosurface.
(3)	Climbing Saucer-Shaped	Both saucer-shape and transgressing elements (Fig. 6b). The facies unit is, thus, in an intermediate stage between saucer-shaped and transgressive. In general, the reflections are as saucer-shaped, but they are typically shallower on one side, resulting in a transgressive appearance. The facies unit is only found locally along the Gjallar Ridge.
(4)	Layer-Parallel Rough	Several layers of dominantly layer-parallel sills with a rough appearance connected by local transgressing segments (Fig. 2). This facies unit is located at 1.5–4 s depth in the central parts of the Vøring Basin.
(5)	Planar Transgressive	Planar, fairly rough, segmented reflections (Fig. 2). The sills are continuous along-strike, forming planar bodies, and are found in the central parts of the sill complex in regions with pre-Cretaceous structural highs (e.g. central Vøring Basin).
(6)	Slightly Saucer-Shaped	Dominantly layer-parallel sills with minor transgressive segments near the tips (Fig. 6). The facies unit is located 1.5–4 s below the palaeosurface and is commonly associated with Layer-Parallel and Saucer-Shaped Rough facies units.
(7)	Fault Block	High-amplitude events inside fault blocks. Sills reflections tend to follow fault planes and stratigraphic weakness zones and the identification of sill intrusions is, therefore, often difficult.
(8)	Smooth Layer-Parallel	Deep, layer-parallel sills with high-amplitude, smooth seismic character and a large degree of continuity (Fig. 6). The facies unit is located at depths ranging from 2.5 to 5 s below the palaeosurface and commonly marks the landward termination of the sill complex.
(9)	Basin-Parallel	Similar to the Smooth Layer-Parallel facies unit, but shows an overall saucer-shape defined by the basin stratigraphy (Figs 2 and 6). The reflections are characterized by high amplitude, smooth seismic character and a large degree of continuity. The facies unit is located at large palaeodepths, ranging from 2.5 to 5 s below the palaeosurface and commonly marks the landward termination of the sill complex.

Table 2. Hydrothermal vent complex statistics

Shape/Size	<2 km	2–5 km	>5 km	Total
Crater	16	33	15	64
Dome	170	51	0	221
Eye	270	171	8	449
n	456	255	23	734

The Top Vent–Top Mound isochron map shows a margin-parallel NE–SW trend expressed by a thin sequence (0.0–0.3 s) in the central and East Vøring Basin, flanked by thicker (0.4–0.8 s) areas along the western parts. There is a remarkable large, thin Top Vent–Top Mound sequence (0.0–0.1 s) in the SW Vøring Basin, continuing SW to the Vøring Transform Margin. Locally, thin sequences are also located above structural highs, e.g. the Gjallar Ridge.

Vent complex statistics

In total, 734 vent complexes were identified in the Vøring and Møre basins (Table 2). The minimum and maximum diameters of the upper part of the vent complexes were 0.4 km and 11 km, respectively. The dominant diameter of the upper part of the vent complexes is 1–2 km, with an average of about 1.5 km. The average diameter for the 2–5 km and >5 km vent complexes are 3.5 km and 7.5 km, respectively. The total relief of the upper part of the vent complexes (Top Vent to Base Vent vertical distance) varies from 0.034 s to 0.50 s, with a mean of 0.13 s. This corresponds to a thickness range of 30–450 m and a mean thickness of 120 m based on an average velocity of 1.8 km s^{-1} derived from well 6607/12-1.

Vent complexes are mainly located in the central and outer parts of the basins. There is a marked difference in number of vent complexes between the Møre and Vøring basins, 133 and 601, respectively (Fig. 7). In general, small and intermediate vent complexes dominate the outer parts of the basins, whereas large vent complexes are found near the inner parts of the basins. Small vent complexes represent more than 60% of all the identified vent complexes and are also the most widespread. Large vent complexes (>5 km) constitute only 3.1% of the total number.

The eye-shaped upper parts dominate, whereas dome-shaped upper parts are also common (Table 2). No large dome-shaped vents were identified. Crater-shaped vents are most common in the inner parts of the Vøring Basin, whereas only two craters have been identified in the Møre Basin.

Mounds are present in the Eocene and Oligocene sequences above the upper part of about 50% of the hydrothermal vent complexes (Figs 9 and 10) and seismic seep anomalies (local high-amplitude events) are interpreted near the seafloor above about 25% of the vent complexes. Inward-dipping reflections are commonly imaged around the conduit zone (about 40%), but outward-dipping reflections are also found (about 10%).

Detectability of hydrothermal vent complexes

The total number of vent complexes formed in the Vøring and Møre basins is probably much higher than the 734 that have been identified in this study. The identification of the vent complexes depends on four main factors: (1) the seismic coverage; (2) the diameter and thickness of the upper parts; (3) the quality of sub-basalt imaging; and (4) local removal of the upper part of the vent complexes by erosion.

Some 20% of the interpreted vent complexes were registered as low quality, indicating that they do not have an easily identified upper part and/or are not associated with the most important characteristic seismic anomalies. Five low-quality vent complexes that were interpreted on the 2D lines are located within the 3D cube area. These vent complexes are well defined on the 3D data.

The interpreted diameter of the upper part of the vent complexes is from 0.4 km to 11 km and the thickness range is 30 m to 450 m. In general, a seismic line has to intersect the average-sized vent complex within 0.75–1 km from the centre to image the structure. The line spacing of the interpreted 2D data is 1 km to 10 km. It is estimated that 2–10 times as many vent complexes as have been identified are present in the Vøring and Møre basins, i.e. 1500 to 7500, with three to five times the identified number as a reasonable range. As a comparison, 15 of the 50 vent complexes that were identified on the 3D data could be identified on the 2D data in the same region.

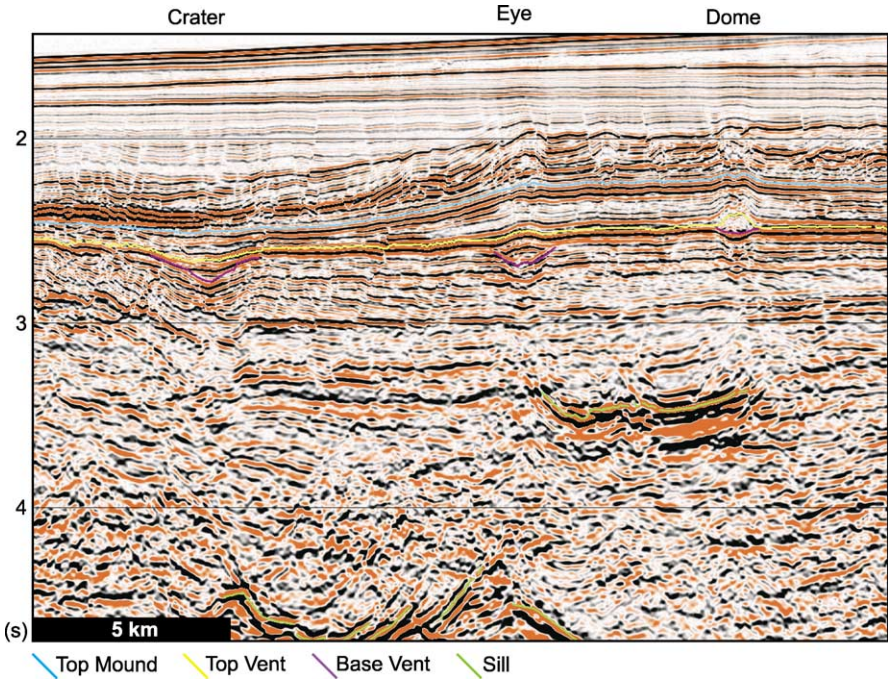

Fig. 9. Seismic profile in the SE Vøring Basin showing the relationships between sill complexes, hydrothermal vent complexes and mounds.

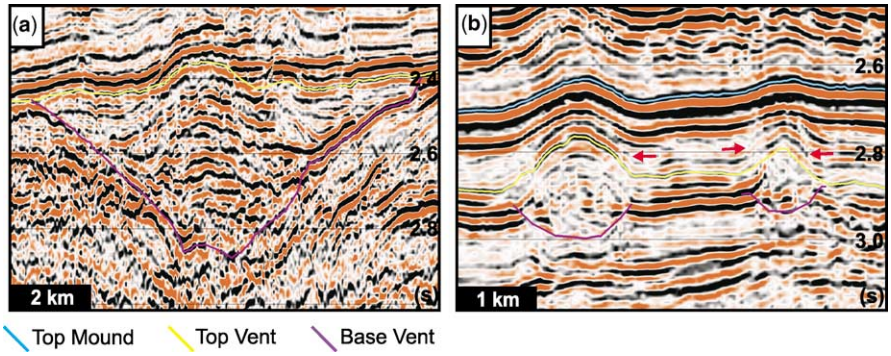

Fig. 10. Seismic examples of the internal reflection configuration in (**a**) crater-shaped vent complexes and (**b**) eye-shaped vent complexes. Note doming of overlying sequences above the vent complexes (mounds).

Vent complexes are probably also hidden beneath the seismically opaque extrusive volcanic rocks, in particular beneath the seismically opaque Inner Flows. Erosion of the upper part of the vent complexes will make them difficult to detect and may have occurred locally in the Vøring and Møre basins (e.g. on the Gjallar Ridge).

Distribution of sill and vent complexes

The seismic profiles show that the formation of hydrothermal vent complexes is closely related to the emplacement of sill intrusions (e.g. Figs 4 and 9). More than 50% of the hydrothermal vent complexes are located above the tip of a sill reflection. The map of the distribution of sill and hydrothermal vent complexes (Fig. 7) shows a well-defined spatial correlation between the presence of sills and vent complexes. The mapping of the vent and sill complexes was done independently, but with seven exceptions all the vent complexes are located in areas where sills are present. Inspection of seismic profiles shows that these seven vent complexes are most likely associated with local intrusions or just slightly offset from a deeper sill complex. No vent complexes were observed above the volcanic extrusive units (e.g. the Inner Flows).

Vent complexes and depth to sills

There is a general correlation between the size and geometry of the upper part of the vent complexes and the depth to the underlying sill intrusion (Table 3). Small, dome-shaped upper parts have the shallowest mean depth to the underlying intrusions, whereas large, crater-shaped upper parts have the largest mean depth to the underlying intrusions. However, it should be noted that there is a fairly large scatter in the data, in particular between small and intermediate size, and eye-shaped and dome-shaped upper parts. However, on the 2D data one can only measure the apparent size of the vent complexes and this measurement uncertainty may partly explain the scatter.

Table 3. Depth between sill reflections and the upper part of hydrothermal vent complexes

	Range (s)	Mean (s)	Comment
Small (<2 km)	0.20–3.74	1.17	Nearly 75% in 0.4–1.6 s range
Intermediate (2–5 km)	0.46–3.79	1.52	Most abundant in the 0.8–1.2 s range
Large (>5 km)	0.90–4.33	2.42	Approximately 75% in 1.6–3.2 s range
Eye	0.20–3.79	1.38	Highest concentration in 0.8–2.0 s range
Dome	0.21–2.65	1.10	Highest concentration in 0.4–1.6 s range
Crater	0.57–4.33	2.00	Evenly distributed in 0.6–3.6 s range

Note: Typical seismic velocity in the Cretaceous sequence: 3–4 km s^{-1}.

Vent complexes and facies units

Figure 11 shows the distribution of the various types of hydrothermal vent complexes in relation to the different sill facies units. Sill facies units 1–3 are saucer-shaped sills located in the outer parts of basins, sill facies units 4–6 are nearly planar intrusions at intermediate depths located in the central parts of the basins, whereas sill facies units 8 and 9 are deep, layer-parallel sills, located in the inner parts of basins. Sill facies unit 7 consists of structurally dependent intrusions.

Most small-sized vent complexes are located above relatively shallow sills (units 1–6). Very few small vent complexes are located above the deep Smooth Layer-Parallel (8) and Basin-Parallel (9) sills. Intermediate-sized vent complexes are present in larger quantities in the eastern part of the basins, i.e. above Smooth Layer-Parallel (8) and Basin-Parallel (9) sills. Large vent complexes are predominantly identified above Slightly Saucer-Shaped (6) or deep Basin-Parallel (9) sills.

Crater-shaped vent complexes are most common in the Slightly Saucer-Shaped (6), Transgressive (5) and Basin-Parallel (9) facies units. Dome-shaped vent complexes are frequently observed above Shallow (1), Layer-Parallel Rough (4) and Slightly Saucer-Shaped (6) facies units, but are rarely seen originating from Smooth Layer-Parallel (8) or Basin-Parallel (9) ones. Eye-shaped vent complexes are associated with all sill facies units, except from intruded Fault Blocks (7). They are most abundant above Saucer-Shaped Rough (2), Layer-Parallel Rough (4), Transgressive (5) and Slightly Saucer-Shaped (6) sill facies units.

Discussion

Sill geometries and emplacement

The seismic facies unit mapping of interpreted sill intrusions reveals several systematic variations in shape and geometry of the sill complexes. (1) Saucer-shaped sills are a fundamental form and are most common in shallow-to-intermediate depths in undeformed basin segments. (2) The deepest parts of the basins are characterized by layer-parallel intrusions. (3) Sill geometries are strongly influenced by structures and heterogeneities such as fault blocks, layering and deformed strata. Similar observations are also common in the field. Saucer-shaped sills are common in the Karoo basin in South Africa, whereas the deep part of the Karoo basin is characterized by dominantly layer-parallel intrusions (e.g. Chevallier & Woodford 1999). In contrast, intrusions in the faulted Mesozoic basins on the Triall Ø, east-central Greenland,

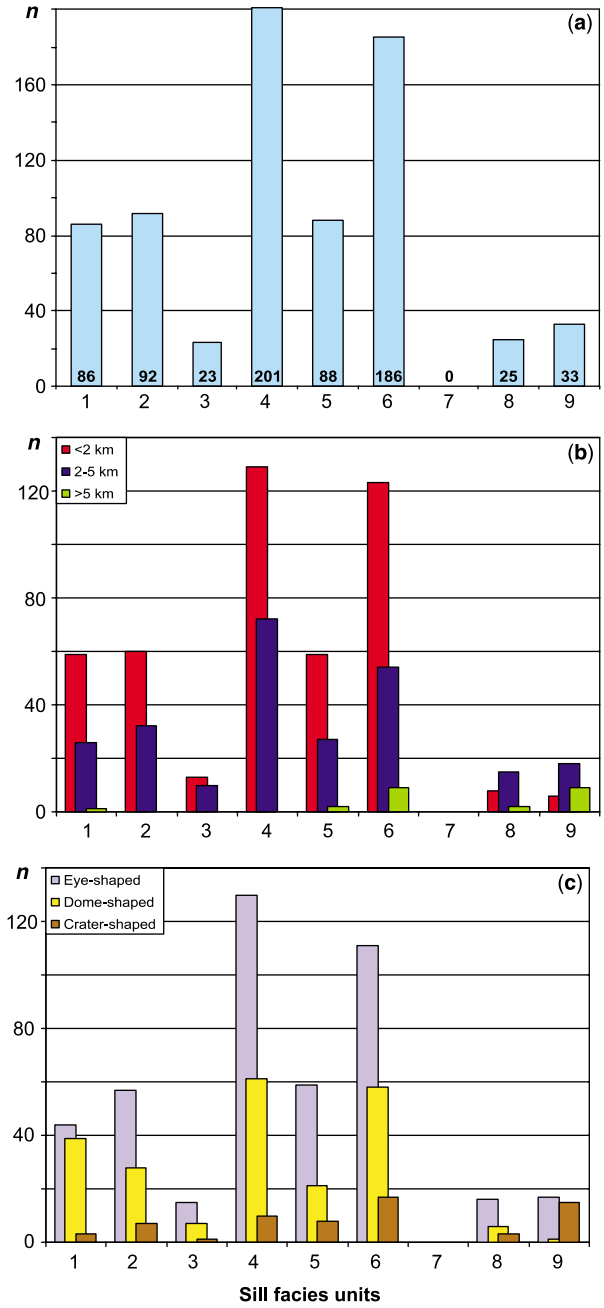

Fig. 11. Distribution of hydrothermal vent complexes in the different sill seismic facies units (Fig. 8; Table 1): (**a**) total number of vent complexes in each facies unit; (**b**) size distribution versus sill facies units; (**c**) geometry of upper part of vent complexes versus sill facies units.

follow fault planes and/or step in the stratigraphy in the vicinity of faults (e.g. Price *et al*. 1997; Planke *et al*. 1999).

Recent numerical modelling by Malthe-Sørenssen *et al*. (2004) shows that saucer-shaped sill intrusions are a fundamental form when the host rock has some elastic strength. The saucers are formed because an anisotropic stress-field develops near the sill tip when the intruding melt is lifting and deforming the overburden, making it easier for the melt to transgress when a critical size is reached. The critical size of the intrusion depends on the host-rock properties and the intrusion depth, but, in general, deep sills must be much larger than shallow sills before they start to transgress. This relationship explains why many deep sills are planar, as they never reach the critical size for transgression. In contrast, different sill geometries are formed in heterogeneous basins or if an external stress-anisotropy is applied. In these cases, the intruding magma will commonly follow weakness zones, such as faults and layering, or it is emplaced perpendicular to the axis of least principal stress. Finally, layer-parallel intrusions are found in unconsolidated sediments, i.e. sediments without any elastic strength (e.g. Planke *et al*. 2000). In this case, the emplacement process is similar to lava-flow emplacement in subaqueous environments.

Hydrothermal vent complex distribution

The seismic data clearly document the causal relationship between sill intrusions and hydrothermal vent complexes. However, hydrothermal vent complexes are not always present in volcanic basins, e.g. on large parts of the Australian NW Shelf (Symonds *et al*. 1998). Three main factors influencing the hydrothermal vent complex abundance in volcanic basins are: (1) the geometry of the sills; (2) the host-rock permeability and composition; and (3) vent complex detectability (size and seismic line spacing).

The formation of hydrothermal vent complexes requires that the local fluid pressure becomes larger than the hydrostatic pressure (Fig. 12). This overpressure build-up can only occur if the pressure build-up is faster than the pressure release, i.e. that the host-rock permeability is small and the pressure generation is fast (Jamtveit *et al*. 2004). Increased pressure around the sills can be caused by boiling of host-rock pore fluids at shallow levels (above a critical depth), metamorphic reactions generating gas and/or degassing of the intruded magma. Clearly, a much higher pressure needs to be generated to fracture 5–10 km of overburden rocks compared with fracturing 1–2 km of overburden rocks when the host-rock properties are similar. If the overburden fractures, then gases will start to rise towards the surface. The rising gases will expand due to decompression and lead to rapid fracturing of the overburden. Seismic data show that the conduit zone is normally vertical and that structural heterogeneities have a minor effect on the structure of the conduit. The rising gas leads subsequently to explosive eruptions at the surface forming blowout craters by removing near-surface unconsolidated sediments and forming the inward-dipping strata around the conduit zone. Field and well-data (Svensen *et al*. 2003; Jamtveit *et al*. 2004) show that the craters are subsequently rapidly in-filled with sediments and commonly no volcanic materials are present in the hydrothermal vent complexes.

The shape of the upper part of the vent complexes is formed by a combination of constructional and compaction processes. Domes may, in some cases, be formed at the seafloor, similar to mud volcanoes in, for example, Azerbaijan (e.g. Planke *et al*. 2003). However, internal reflection configuration and well data show that the upper part of the vent complexes mainly consist of craters and that the observed shapes are a function of the basin compaction history. Well data from 6607/12-1 on the mid-Norwegian margin suggest that a high fluid pressure has been maintained in the vent complex since its formation. The convex shape of the upper part of this vent complex was formed because the crater infill has been compacted less than the surrounding strata, i.e. the structure was formed by compaction processes and not by eruption processes.

Care has been taken to keep the interpretation of the Top Vent and Top Mound horizons at the same stratigraphic level using limited well control in the outer Vøring Basin. More than 95% of the upper part of the hydrothermal vent complexes terminate at the Top Vent horizon. The hydrothermal vent complex drilled by 6607/12-1 can be dated by biostratigraphy to 55.0 Ma to 55.8 Ma (Svensen *et al*. 2004) and the Top Vent horizon is correspondingly dated as the Top Paleocene horizon. The Top Vent reflection correlates with the Inner Flows, but no vent complexes are identified in, or above, the volcanic extrusive cover. This observation suggests that the intrusive event terminated just before the main volcanic event. However, the 20 vent complexes terminating in the Upper Paleocene sequence in the Møre Basin and the presence of volcanic flows below the Top Vent horizon in the Møre Basin and

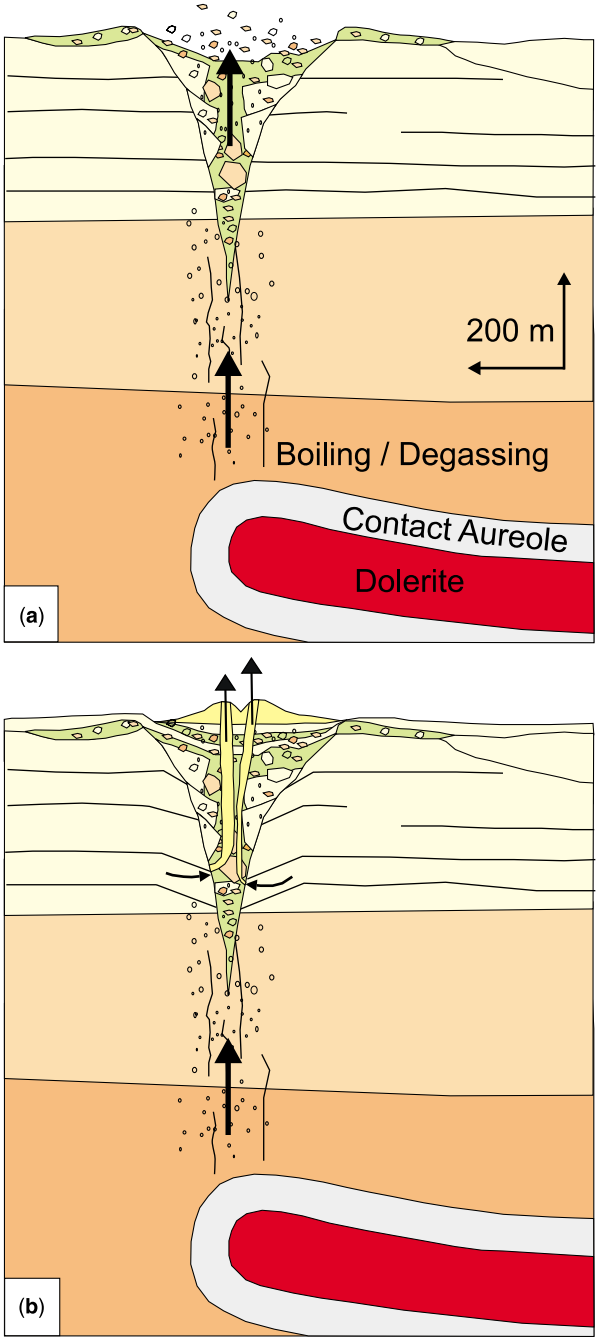

Fig. 12. Sketch showing the development of a hydrothermal vent complex. (**a**) Boiling of pore fluids or gas formation (degassing of magma, metamorphic reactions) cause fluid pressure build-up and explosive formation of a cone-shaped hydrothermal vent complex. The initial fluid expulsion is associated with fragmentation and generation of hydrothermal breccias. (**b**) Subsequently, large (several metres across) pipes of fluidized sandstone cross-cut the brecciated rocks. Smaller hydrothermal pipes (cm-size) form during later reworking of the cone structure, following a reduction in fluid pressure gradients (from Jamtveit *et al.* 2004).

the South Vøring Basin, is evidence of a minor magmatic event prior to the main break-up volcanic episode.

Mound structures and seep

The Top Mound horizon is not as well dated as the Top Vent horizon. It correlates with a major Eocene–Miocene unconformity in 6607/12-1 and is tentatively assigned an intra-Oligocene age. The Top Mound dome structures are quite different from the upper part of the hydrothermal vent complexes as the seismic reflections are mainly upward doming and no inward-dipping events are found. The mounds are not only present above the hydrothermal vent complexes, but also above the termination of deep Mesozoic/Early Tertiary faults on, for example, the Gjallar Ridge. The mounds are also sometimes associated with seismic seep anomalies all the way up to the seafloor (disturbed seismic chimneys and local high-amplitude seismic anomalies). The mound structures are interpreted here as seep anomalies, probably formed by biological activity feeding on methane and other fluids seeping through the vent complexes or other weakness zones. The seep anomalies further indicate that the hydrothermal vent complexes have a long-term impact on the fluid migration pathways in pierced basins.

Conclusions

Regional seismic mapping in the Vøring and Møre basins off mid-Norway has documented an extensive Palaeogene sill complex with an extent of at least 80 000 km^2. The sheet intrusions are saucer-shaped in undeformed basin segments and the size of the saucers becomes larger with increasing emplacement depth. More varied intrusion geometries are found in structured basin segments, where the melt was emplaced along weakness zones such as fault planes and along stratigraphic layers. The total volume of the intrusive complex is estimated to be in the range $0.9–2.8 \times 10^4$ km^3. The volume is difficult to calculate, as both thickness measurements and, in particular, the seismic interpretation of deep intrusions, have a low reliability.

734 hydrothermal vent complexes have been identified and it is estimated that as many as at least 2–3000 vent complexes are present in the Vøring and Møre basins. The vent complexes are located above sills and were formed as a direct consequence of the intrusive event. The vent complexes were formed mainly by explosive eruption of gases, liquids and sediments, forming craters at the seafloor. Constructional domes, or possibly mud volcanoes, are also present. The largest craters (>5 km in diameter) are located in regions with deep sill complexes, whereas small dome- and eye-shaped upper parts are located above shallow sill complexes. Mounds and seismic seeps located above the hydrothermal vent complexes show that the vent complexes are re-used for vertical fluid migration a long time after their formation.

Most of the upper part of the vent complexes (>95%) is located at the Top Paleocene level. The intrusive event occurred just prior to, or during, the initial phase of massive break-up volcanism (55.0–55.8 Ma). There is also evidence for a minor Late Paleocene volcanic event documented by the presence of 20 vent complexes terminating in the Upper Paleocene sequence and the presence of Inner Flows within the Paleocene sequence. It is not possible to subdivide the intrusive episode into more than these two main events.

This contribution has benefited from discussions with many people, in particular the participants on the 'Petroleum Implications of Sill Intrusions' project and collaborators in South Africa (L. Chevallier, J. Marsh). Seismic data were supplied by TGS-NOPEC, whereas VoxelVision carried out the 3D seismic imaging. Constructive reviews from B. Bell and K. Thomson are appreciated.

References

Bell, B. R. & Butcher, H. 2002. On the emplacement of sill complexes: evidence from the Faroe–Shetland Basin. *In*: Jolley, D. W. & Bell, B. R. (eds) *The North Atlantic Igneous Province: Stratigraphy, Tectonic, Volcanic and Magmatic Processes*. Geological Society, London, Special Publications, **197**, 307–329.

Berndt, C., Skogly, O. P., Planke, S., Eldholm, O. & Mjelde, R. 2000. High-velocity breakup-related sills in the Vøring Basin, off Norway. *Journal of Geophysical Research*, **105**, 28443–28454.

Berndt, C., Planke, S., Alvestad, E., Tsikalas, F. & Rasmussen, R. 2001. Seismic volcanostratigraphy of the Norwegian Margin: constraints on tectonomagmatic break-up processes. *Journal of the Geological Society, London*, **158**, 413–426.

Blystad, P., Brekke, H., Færseth, R. B., Larsen, B., Skogseid, J. & Tørudbakken, B. 1995. *Structural elements of the Norwegian continental shelf, Part II: The Norwegian Sea region*. The Norwegian NPD-bulletin 8, Petroleum Directorate.

Brekke, H. 2000. The tectonic evolution of the Norwegian Sea Continental Margin with emphasis on the Vøring and Møre Basins. *In*: Nottvedt, A. (ed.) *Dynamics of the Norwegian Margin*. Geological Society, London, Special Publications, **167**, 327–378.

Bugge, T., Prestvik, P. & Rokoengen, K. 1980. Lower Tertiary volcanic rocks off Kristiansund, mid-Norway. *Marine Geology*, **35**, 277–286.

Chevallier, L. & Woodford, A. 1999. Morpho-tectonics and mechanism of emplacement of the dolerite rings and sills of the western Karoo, South Africa. *South African Journal of Geology*, **102**, 43–54.

Davis, R., Bell, B. R., Cartwright, J. A. & Shoulders, S. 2002. Three-dimensional seismic imaging of Palaeogene dike-fed submarine volcanoes from the northeast Atlantic margin. *Geology*, **30**, 223–226.

Eldholm, O., Thiede, J. & Taylor, E. 1989. Evolution of the Vøring volcanic margin. *ODP Scientific Results*, **104**, 1033–1065.

Gernigon, L., Ringenbach, J. C., Planke, S., Le Gall, B. & Jonquet-Kolstø, H. 2003. Extension, crustal structure and magmatism at the outer Vøring Basin, Norwegian margin. *Journal of the Geological Society, London*, **160**, 197–208.

Gibb, F. G. F. & Kanaris-Sotiriou, R. 1988. The geochemistry and origin of the Faeroe–Shetland sill complex. *In*: Morton, A. C. & Parson, L. M. (eds) *Early Tertiary Volcanism and the Opening of the NE Atlantic*. Geological Society, London, Special Publications, **39**, 241–252.

Hjelstuen, B., Eldholm, O. & Skogseid, J. 1999. Cenozoic evolution of the northern Vøring margin. *Geological Society of America Bulletin*, **111**, 1792–1807.

Jamtveit, B., Svensen, H., Podladchikov, Y. & Planke, S. 2004. Hydrothermal vent complexes associated with sill intrusions in sedimentary basins. *In*: Breitkreuz, C. & Petford, N. (eds) *Physical Geology of High-Level Magmatic Systems*. Geological Society, London, Special Publications, **234**, 233–241.

Larsen, H. C. & Marcussen, C. 1992. Sill-intrusions, flood basalt emplacement and deep crustal structure of the Scoresby Sund region, East Greenland. *In*: Morton, A. C. & Parson, L. M. (eds) *Early Tertiary Volcanism and the Opening of the NE Atlantic*. Geological Society, London, Special Publications, **39**, 95–114.

Malthe-Sørenssen, A., Planke, S., Svensen, H. & Jamtveit, B. 2004. Formation of saucer-shaped sills. *In*: Breitkreuz, C. & Petford, N. (eds) *Physical Geology of High-Level Magmatic Systems*. Geological Society, London, Special Publications, **234**, 215–227.

Menzies, M. A., Klemperer, S. L., Ebinger, C. J. & Baker, J. 2003. Characteristics of volcanic rifted margins. *Geological Society of America*, *Special Paper*, **362**, 1–14.

Planke, S. & Alvestad, E. 1999. Seismic volcanostratigraphy of the extrusive breakup complexes in the northeast Atlantic: Implications from ODP/DSDP drilling. *ODP Scientific Results*, **163**, 3–16.

Planke, S. & Myklebust, R. 1999. Når seismikken kommer til kort. *GEO*, Trondheim, 20–21.

Planke, S., Steen, Ø., Gisselø, P., Skogly, O. P. & Skogseid, J. 1999. Outcrops on Traill Ø, East Greenland, guiding seismic interpretation of sill complexes in Mesozoic basins in the NE Atlantic realm. *In*: *The role of geological fieldwork in hydrocarbon exploration and production*. CASP Publication, London, 56–57.

Planke, S., Symonds, P., Alvestad, E. & Skogseid, J. 2000. Seismic volcanostratigraphy of large-volume basaltic extrusive complexes on rifted margins. *Journal of Geophysical Research*, **105**, 19335–19351.

Planke, S., Svensen, H., Hovland, M., Banks, D. A. & Jamtveit, B. 2003. Mud and fluid migration in active mud volcanoes in Azerbaijan. *Geo-Marine Letters*, **23**, 258–268.

Price, S., Brodie, J., Whitham, A. & Kent, R. 1997. Mid-Tertiary rifting and magmatism in the Triall Ø region, East Greenland. *Journal of the Geological Society, London*, **154**, 419–434.

Sandwell, D. T. & Smith, W. H. F. 1997. Marine gravity anomaly from Geosat and ERS 1 satellite altimetry. *Journal of Geophysical Research*, **102**, 10039–10054.

Skogly, O. P. 1998. *Seismic characterization and emplacement of intrusives in the Vøring Basin* PhD thesis, University of Oslo.

Skogseid, J., Pedersen, T., Eldholm, O. & Larsen, B. T. 1992. Tectonism and magmatism during NE Atlantic continental break-up: the Vøring Margin. *In*: Storey, B. C., Alabaster, T. & Pankhurt, R. J. (eds) *Magmatism and the Causes of Continental Break-up*. Geological Society, London, Special Publications, **68**, 305–320.

Smallwood, J. & Maresh, J. 2002. The properties, morphology and distribution of igneous sills: modeling, borehole data and 3D seismic from the Faroe–Shetland area. *In*: *The North Atlantic Igneous Province: Stratigraphy, Tectonic, Volcanic and Magmatic Processes*. Geological Society, London, Special Publications, **197**, 271–306.

Svensen, H., Jamtveit, B., Planke, S. & Pedersen, T. 2003. Seep carbonate formation controlled by hydrothermal vent complexes: a case study from the Vøring volcanic basin, the Norwegian Sea. *Geo-Marine Letters*, **23**, 351–358.

Svensen, H., Planke, S., Malthe-Sørenssen, A., Jamtveit, B., Myklebust, R., Rasmussen, T. & Rey, S. S. 2004. Explosive release of methane from a volcanic basin as a mechanism for the initial Eocene global warming. *Nature*, **429**, 542–545.

Symonds, P. A., Planke, S., Frey, Ø. & Skogseid, J. 1998. Volcanic development of the Western Australian continental margin and its implications for basin development. *In*: Purcell, P. G. & Purcell, R. R. (eds) *The Sedimentary Basins of Western Australia 2: Proceedings of Petroleum Exploration Society of Australia Symposium*, Perth, 33–54.

Vail, P. R. & Mitchum, R. M. 1977. Seismic stratigraphy and global changes of sea level, 1, Overview. *In*: *American Association of Petroleum Geologists*, Memoir, **26**, 21–52.

Verhoef, J., Roest, R., Macnab, R. & Arkani-Hamad, J. 1996. Magnetic anomalies of the arctic and North Atlantic oceans and adjacent land areas. *GSC Atlantic Open File 3125a*, Dartmouth, Canada.

White, R. S., Smallwood, J. R., Fliedner, M. M., Boslaugh, B., Maresh, J. & Fruehn, J. 2003. Imaging and regional distribution of basalt flows in the Faeroe–Shetland basin. *Geophysical Prospecting*, **51**, 215–231.